

Simulations of background sources in AMoRE-I experiment

A. Luqman^a, D.H. Ha^a, J.J. Lee^b, E.J. Jeon^{c,*}, H.S. Jo^c, H.J. Kim^a,
Y.D. Kim^c, Y.H. Kim^{c,d}, V.V. Kobychiev^e, H.S. Lee^c, H.K. Park^c, K. Siyeon^b,
J.H. So^c, V.I. Tretyak^e, Y.S. Yoon^{c,*}

^a*Department of Physics, Kyungpook National University, DaeGu 41566, Korea*

^b*Department of Physics, Chung-Ang University, Seoul, Korea*

^c*Center for Underground Physics, Institute for Basic Science, Daejeon 34047, Korea*

^d*Korea Research Institute of Standards and Science, Daejeon 34113, Korea*

^e*Institute for Nuclear Research, MSP 03680 Kyiv, Ukraine*

Abstract

The first phase of the Advanced Mo-based Rare Process Experiment (AMoRE-I), an experimental search for neutrinoless double beta decay ($0\nu\beta\beta$) of ^{100}Mo in calcium molybdate (CMO) crystal using cryogenic techniques, is in preparation at the YangYang underground laboratory (Y2L) in South Korea. A GEANT4 based Monte Carlo simulation was performed for background estimation in the first-phase the AMoRE-I detector and shield configuration. Background sources such as ^{238}U , ^{232}Th , ^{235}U , and ^{210}Pb were simulated from inside the crystals, surrounding materials, outer shielding walls of the Y2L cavity. The estimated background rate in the region of interest was estimated to be $<1.5 \times 10^{-3}$ counts/keV/kg/yr (ckky). The effects of random coincidences between background and two-neutrino double beta decay of ^{100}Mo were estimated as a potential background source and its estimated rate was $<2.3 \times 10^{-4}$ ckky.

Keywords: Background, simulation, neutrinoless double beta decay

*Corresponding author

Email addresses: ejjeon@ibs.re.kr (E.J. Jeon), ysy@ibs.re.kr (Y.S. Yoon)

1. Introduction

As of today, on the basis of results from a number of neutrino oscillation experiments, it is known that neutrinos have mass. However, their absolute mass scale is still not known [1, 2, 3]. The half-life of neutrinoless double beta decay ($0\nu\beta\beta$) of certain nuclei is related to the effective Majorana neutrino mass, and the investigation of neutrinoless double beta decays is the only practical way to determine the absolute neutrino mass scale and the nature of the neutrino such as Majorana or Dirac particle [3]. The Advanced Mo-based Rare Process Experiment (AMoRE) [4] is an experimental search for neutrinoless double beta decay of ^{100}Mo nuclei using CaMoO_4 (CMO) scintillating crystals operating at milli-Kelvin temperatures and is planned to operate at the YangYang underground laboratory (Y2L) in South Korea. The AMoRE experiment will run in a series of phases [5]; the first phase of the experiment (AMoRE-I) will use a ~ 5 kg (possibly, up to 10 kg) array of CMO crystals. The goal of a background level for AMoRE-I is 0.002 counts/keV/kg/yr (ekky) in the region of interest (ROI), 3.034 ± 0.01 MeV. Radiation originating within the CMO crystals are known to be the dominant source of backgrounds [6]. These include activities from radioisotopes contained in the ^{238}U , ^{232}Th , and ^{235}U decay chains from materials in the nearby detector system and the outer lead shielding box that produce signals in the crystals. Backgrounds from more remote external sources such as the surrounding rock material and cement floor are considered. Random coincidences of radiation from different background sources with two-neutrino double beta ($2\nu\beta\beta$) decay of ^{100}Mo in CMO is known as a possible background source in the ROI [7, 8]. In this paper we report estimates of background counting rates due to the above mentioned background sources by performing simulations that investigate the effects of dominant background sources on the measured energy spectrum near the ROI.

2. The AMoRE-I Experiment

2.1. The geometry for detector simulation

30 The detector geometry used for the AMoRE-I simulation includes the CMO crystals, the shielding layers internal to the cryostat, the external lead shielding box, and the outer rock walls of the Y2L cavity. Each crystal has a cylindrical shape with a 4.5 cm diameter, 4.5 cm height, and a mass of 310 g. The total mass of crystals is 10.9 kg, originated from initial design of AMoRE-I experiment. The
35 thirty-five crystals are arranged in seven vertical columns, each with five crystals stacked coaxially, with one center column surrounded by six external ones. The side, bottom and a ring shape of top surfaces of each crystal are covered by a 65 μ m-thick Vikuiti Enhanced Specular Reflector film (former VM2000). Each crystal is mounted in copper frames, which have very complicated design in
40 reality, but, in the simulation, a simplified design of the CMO supporting copper frames with corresponding mass is used, as shown in Fig. 1. Ge wafer and its copper frames are located above each crystal and below the lowest crystal. More detailed detector description is found elsewhere [5, 9].

This whole crystal assembly is enclosed in a cylindrical 2-mm-thick lead
45 superconducting magnetic shielding tube with top and bottom discs, which is made of ultra-low activity, ancient lead. A 1-cm-thick copper plate and 10-cm-thick lead plate (diameter of 40.8 cm and mass of 148.3 kg) are located in series just above the CMO crystal assembly, to attenuate backgrounds from materials above crystals inside the cryostat, such as wires, temperature sensors,
50 heaters, G10 fiberglass tubes, and stainless steel tubes. The crystal assembly is placed inside of four concentric copper cylinders with a total Cu thickness of 10 mm, all within an outer stainless-steel vacuum cylinder that is 5 mm thick, as shown in Fig. 2. Sequential top plates of shields are connected with G10 fiberglass tubes, which were made of woven fiberglass material with 12
55 cm-height, 2.5 cm-diameter (~ 25 g) and they are known as a material with high radioactive background. In this simulation configuration, simple top plates and G10 fiberglass tubes took into account in the detector geometry. Realistic

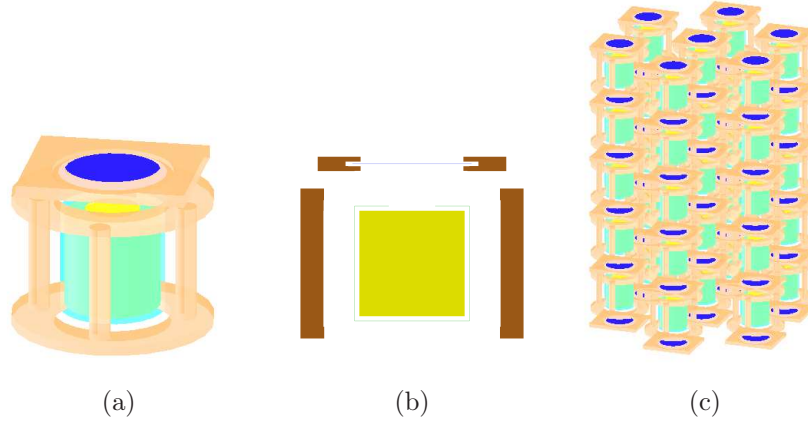


Figure 1: (a) CMO crystal (yellow) with Vikuiti reflector (light green) and CMO supporting copper frame (brown). On the top of reflector was open for a Ge wafer. (b) Vikuiti reflector surrounds each crystal except for center area on the top. (c) 35 CMO crystals were stacked up 5 layers and 7 columns.

structures and features will be positioned on each of the top plates for use in future simulations.

60 The cryostat is located inside a 15-cm-thick external lead shield, a total mass of ~ 15.6 ton. The top plate of the lead shield, covering an area of $150 \times 150 \text{ cm}^2$, is separated and placed ~ 50 -cm above the top of the cryostat, which is a space for pipe and valve for the cryostat in the real detector system. For radiations from the rock walls surrounding the experimental enclosure, the simulation uses
65 a 50-cm-thick spherical rock shell, which is an optimized thickness for saturated escaping γ -rays. For radiations from the laboratory environment such as the cement floor, the laboratory walls and ceiling, and Iron supporting system, the simplified design were implemented into geometry as shown in Fig. 3.

2.2. Simulation method

70 We have performed simulations using the GEANT4 Toolkit [10]. In internal or external materials, expected radioactive sources such as full decay chain of

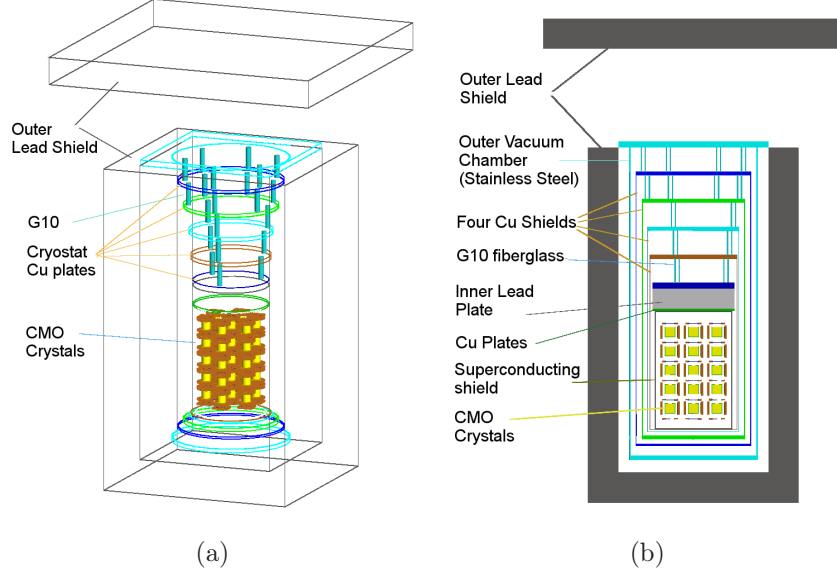


Figure 2: Outside the cryostat, a 15 cm-thick outer lead shield is located. The cryostat is composed of a stainless steel shield and four Cu shields. Top plates of cryostat shields are connected to G10 fiberglass tubes (a). All the way inside the cryostat, the inner lead plate (gray) on the top of Cu plate is located above crystals. The 2-mm-thick superconducting lead shield surrounds crystals inside the cryostat.

^{238}U , ^{232}Th , and ^{235}U were simulated. Generally, most decay sources and their daughters were considered to be in equilibrium state, thus all related activities within the chains are simply equal to ^{238}U , ^{232}Th , and ^{235}U activities multiplied by the branching ratios for decay of the daughter isotopes. However, for ^{238}U decays inside crystals, broken decay chain was considered by measured ^{238}U and ^{222}Rn concentrations separately. For radiations from rock, instead of ^{40}K and full decay chain simulation of ^{238}U and ^{232}Th nuclei, the highest energy γ such as 1.46, 1.87, and 2.61 MeV, respectively, were simulated at a rock shell, since daughter nuclei, α , and β cannot penetrate the lead shield and the cryostat, made of stainless steel and copper shields.

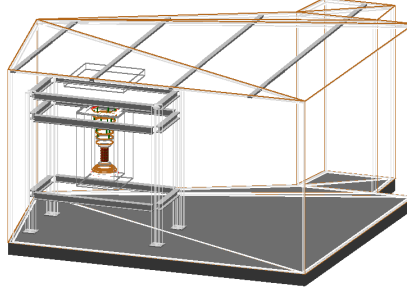


Figure 3: Cement floor, laboratory walls, ceiling of Y2L laboratory. Hollow steel poles (green) are on the wall and ceiling and between poles were filled with glass wool. Inner and outer of steel poles were covered by plaster board and steel plate in series.

Each simulated event includes deposits inside crystals within an event window of 100 ms when a decay occurs, which based on a few times of typical pulse width ($\sim 20\text{-}30$ ms) in cryogenic measurements [9]. Sometimes decays with relatively short half lifetime such as, ^{212}Po decay with a half lifetime of 300 ns, and the followed decay will appear in the same event, called pileup events, and they were treated within one event in simulated event. Furthermore, effect of random coincidence of ^{100}Mo $2\nu\beta\beta$ decay events and other radioactive sources inside crystals were estimated by convolution technique. For random coincidence rate calculation, ^{100}Mo $2\nu\beta\beta$ decay events were generated using an event generator, DECAY0 program [11] and those events were used as input particles in our simulation package with AMoRE-I detector configuration to get a distribution of ^{100}Mo $2\nu\beta\beta$ decay inside CMO crystals.

3. Analysis

Radioactive sources were simulated in the following materials, known as dominant background sources: (i) First, the internal background in CMO crystals (ii) Second, backgrounds from materials in detector system, including CMO

supporting copper frame, Vikuiti reflector, superconducting lead shield, Cu plate under internal lead, internal lead plate, G10 fiberglass tubes, and outer lead shielding box (iii) Third, backgrounds from rock material and surrounding underground laboratory. Then, we estimate an anti-coincidence rate and random coincidence rate with ^{100}Mo $2\nu\beta\beta$ decay.

The anti-coincidence rate is estimated from an event rate in ROI in one crystal, called a single hit event, while events with hits on more than one crystal are rejected because they are obviously from radioactive decays. The single hit events are surface α events, β - α pileup events, and β -like (β or γ) events. First, the surface α -events from crystals or near-by materials can leave deposited energy in the crystals in a continuum distribution up to Q-value (see Section 3.2.1 and Ref. [12]), which possibly appear in ROI. Those α signal are distinguished from β and γ signals by pulse shape discrimination (PSD) and a separation power of 7.6σ between α and β/γ events were reported [13]. We assumed that α event rejection power is 99.9999 % in this estimation. Second, the β - α pileup events are from decays of ($^{212}\text{Bi}+^{212}\text{Po}$) in ^{232}Th decay chain, with half lifetime of 300 ns, and decays of ($^{214}\text{Bi}+^{214}\text{Po}$) in ^{238}U decay chain, with a half lifetime of 164 μs . When β - α pileup events occurred near the surface of crystal or near-by materials, events with a fraction of α Q-value and β -energy possibly appear in ROI. These β - α pileup events from ^{238}U and ^{232}Th chains can be rejected by PSD analysis with a rejection power of 99 %, which was reported clear separation between α and β -like events with a prototype detector [13, 5]. In this estimation, 90 % rejection efficiency ($\sim 1.6\sigma$) was assumed, conservatively. After surface α rejection, remaining anti-coincidence rate is mainly β -like single hit event rate in ROI. Further rejection scheme for β -like single hit events will be discussed in Section 3.1.1.

Random coincidence events are originated from any two pulse signals, while β - α pileup events are from two consecutive decays with relatively short half lifetime. When two random signals occurred within a time resolution, they might considered as one pulse, which could be possible background source in ROI. Random coincidence event rate within a time resolution of 0.5 ms [14] were

estimated by convolution of two background spectra. The Random coincidence
130 rate includes not only randomly coincident events by two ^{100}Mo $2\nu\beta\beta$ decays,
but those by a ^{100}Mo $2\nu\beta\beta$ decay and another decay from other background
sources (see Section 3.1.2).

Activities of ^{238}U , ^{232}Th , and ^{235}U which were used to normalize the simu-
lation results, were measured by germanium counting and inductively coupled
135 plasma mass-spectroscopy (ICP-MS) technique. The High Purity Ge (HPGe)
measurements were performed at Y2L. The ICP-MS measurements were all
performed by the KAIST Analysis Center for Research Advancement (KARA),
South Korea. The activity of backgrounds in a CMO crystal was measured by
low temperature detector technique [13]. Activity of some materials were from
140 published references. The concentration of materials are listed in the following
section. Here, the activities from bulk and surface contamination are considered
as uniform for crystals and near-by materials. The surface alpha events might
be independent source from bulk [15].

3.1. Internal background in CMO crystals

145 3.1.1. Background rate due to sources inside CMO crystals

The activities inside crystals, listed in Table 1, were from a recent mea-
surements of a CMO crystal [16], except an activity of ^{232}Th . For the activity
of ^{232}Th , a conservative upper limit were used. Using activities of radioac-
tive sources in crystals, event rates in ROI were normalized to the unit of
150 counts/keV/kg/yr (ckky). Fig. 4 shows deposited energy distributions in CMO
crystals for total single-hit event rate, β - α pileup rate, and β -like event rate
exclusively.

Table 1: Activities based on a CMO crystal measurement [16] [mBq/kg]

	^{210}Pb	^{238}U	$^{226}\text{Ra}(^{222}\text{Rn})$	^{232}Th	$^{235}\text{U}(^{211}\text{Bi})$
Activity	7.3	0.98	0.065	<0.05	0.47

As shown in Fig. 4, β -like events from ^{208}Tl decay in ^{232}Th chain is a candidate of dominant source in ROI, but they can be rejected using time correlations with the α signal from the preceding $^{212}\text{Bi} \rightarrow ^{208}\text{Tl}$ α decay, called α -tagging method. Rejection of all events occurring within 30 mins after an α event with 6.207 MeV in the same crystal, results in a 97.4% veto efficiency for ^{208}Tl -induced β events in the ^{100}Mo $2\nu\beta\beta$ signal region, while introducing $\sim 1\%$ dead-time.

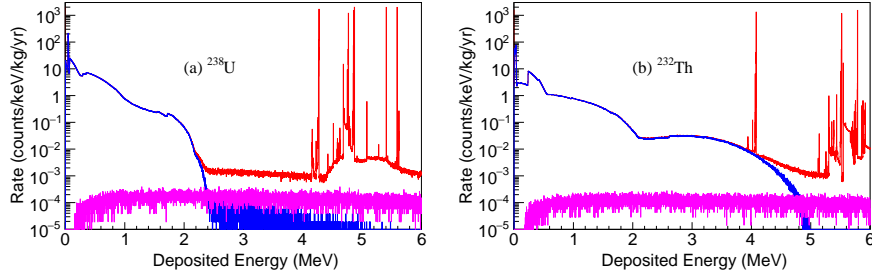


Figure 4: Single hit event rate distribution from (a) ^{238}U and (b) ^{232}Th inside crystals for total events (red) including α s, β - α pileup events (pink), and β -like event exclusively (blue). The difference between total rate (red) and sum of the others is α particle event rate.

3.1.2. Random coincidence rate of two ^{100}Mo $2\nu\beta\beta$ decays

The $2\nu\beta\beta$ decay in a CMO approaches zero rate at the end-point energy, but random coincidence of these events can sum together (pileup) creating backgrounds for the $0\nu\beta\beta$ signal. The random coincidence of two ^{100}Mo $2\nu\beta\beta$ decays in an energy range, ΔE , can be expressed as [17],

$$R_{rc} = \tau \cdot R_0^2 \cdot \varepsilon = \tau \left(\frac{\ln 2 \cdot N}{T_{1/2}^{2\nu 2\beta}} \right)^2 \varepsilon \quad (1)$$

where N is the number of ^{100}Mo decays and ε is the probability of appearing events in the ΔE interval, which was evaluated by convolution of two simulated distribution here. The expected rate of $2\nu\beta\beta$ decay in a single CMO crystal

with ~ 306 g is 0.0028 counts/s, which is one double beta decay event per ~ 6 mins.

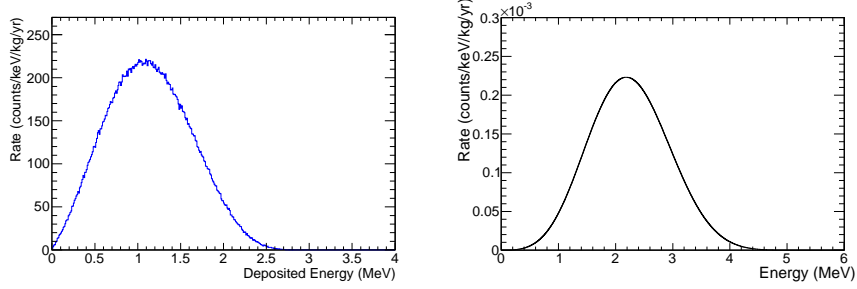


Figure 5: The energy distribution of ^{100}Mo $2\nu\beta\beta$ decay (left) and random coincidences of two $2\nu\beta\beta$ decays of ^{100}Mo (right). The random coincidence spectrum is derived by convolution of the $2\nu\beta\beta$ spectrum, and was normalized according to the $2\nu\beta\beta$ rate assuming an 0.5 ms coincidence window.

170 When 5×10^8 $2\nu\beta\beta$ events were simulated in the CMO crystals, ~ 99 % of events have energy deposits in one crystal (single-hit events) and the remaining events (< 1 %) produced hits in multiple crystals. The random coincidence rate of two $2\nu\beta\beta$ decays was calculated by convolving two single-hit $2\nu\beta\beta$ decay energy distributions (see Fig. 5) and the accidental rate in the coincidence window
175 is 1.2×10^{-4} ckky in the ROI.

Random coincidence rates of ^{100}Mo $2\nu\beta\beta$ decay and each radioactive background source inside CMO crystals such as ^{210}Pb , ^{238}U , ^{232}Th , ^{40}K , ^{235}U were calculated as well. The concentration was from measurements, shown in Table 1, and concentration of ^{40}K was assumed as 1 mBq/kg [18, 19]. The sum of random coincidence rates is Mo $2\nu\beta\beta$ decays and other nuclei was 7.80×10^{-6} ckky.
180 In the same way, the random coincidence rates of two radioactive background sources inside CMO crystals were calculated and the sum of rates between two background sources were 2.23×10^{-8} ckky.

3.2. Backgrounds from materials in detector system

3.2.1. Backgrounds from materials inside and on the cryostat

Activity of radioactive sources in Vikuiti reflector, measured by HPGe at Y2L [20], was 0.91 mBq/kg and 0.48 mBq/kg for ^{238}U (^{226}Ra) and ^{232}Th (^{228}Th), respectively. The CMO supporting copper frame was made of NOSV grade copper from Aurubis Co. and reported concentration of NOSV copper [21] was shown in Table 2. We purchased T2FA lead bricks from Lemer Pax with a certified activity of ^{210}Pb , 0.3 Bq/kg for inner lead plate and superconducting lead shield. Activity of ^{238}U and ^{232}Th in G10 fiberglass tubes was measured by ICP-MS, as shown in Table 3, which is in the similar order of the reported results [22]. The activity of ^{238}U and ^{232}Th on the outer vacuum chamber, made of stainless steel, was from a reference[6], and measurement of stainless steel activity is planned.

Table 2: Activities of ^{238}U and ^{232}Th in Vikuiti reflector [20] and NOSV copper [21]

	^{238}U (^{226}Ra)	^{232}Th (^{228}Th)
Vikuiti Reflector	<0.91 mBq/kg	<0.48 mBq/kg
CMO supporting copper frame	<16 $\mu\text{Bq/kg}$	<25 $\mu\text{Bq/kg}$

The estimated α and β - α pileup event rates of ^{238}U and ^{232}Th contaminants in the Vikuiti reflecting foils were in the order of 10^{-4} ckky, but they can be rejected by PSD analysis, like internal background events. The β -like event rate is in the order of 10^{-4} ckky in ROI. The estimated α and β - α pileup event rate in CMO supporting copper frame were in the order of 10^{-5} ckky. Since each crystal is surrounded by Vikuiti reflector except top center area, α -particles and β from CMO supporting copper frame rarely reach to crystals directly and β -like events, mostly γ -rays, make signals on crystals, as shown in Fig. 6.

The effect of radioactive sources from superconducting (SC) lead shield and

Table 3: Concentrations and activities of radioactive sources in materials inside and on the cryostat

	^{210}Pb	^{238}U	^{232}Th
Superconducting lead shield	0.3 Bq/kg	1 ppt	1 ppt
Cu plate under inner lead	-	$<16 \mu\text{Bq/kg}$	$<25 \mu\text{Bq/kg}$
Inner lead plate	0.3 Bq/kg	1 ppt	1 ppt
G10 fiberglass tubes	-	1732 ppb	12380 ppb
Stainless steel shield		$<0.2 \text{ mBq/kg}$	$<0.1 \text{ mBq/kg}$
Outer lead shield	$<59 \text{ Bq/kg}$	6.9 ppt	3.8 ppt

other materials, placed outer than the SC lead shield, were from β -like events, mainly γ s, like CMO supporting copper frames. When no events were found in ROI for thousands of exposure, upper limit (90% C.L.) was estimated and the limit were to be in the order of 10^{-5} ckky by increasing statistics, as shown in Fig. 7.

Random coincidence rates of β -like events from materials inside the cryostat with ^{100}Mo $2\nu\beta\beta$ decay were in the order of $\sim 10^{-7} - 10^{-9}$ ckky for CMO supporting copper frame, SC lead shield, Cu plate, internal lead plate, which are less than random coincidence rate of two ^{100}Mo $2\nu\beta\beta$ decay inside the crystals.

3.2.2. Backgrounds from lead shielding box outside the cryostat

Main concern of the lead shielding box was the random coincidence events between ^{100}Mo $2\nu\beta\beta$ decay and γ s from ^{210}Pb , which were enclosed into the 16 tons of the lead shield box. For the lead shielding box, the JR Goslar lead bricks were purchased with a ^{210}Pb certification and measured activities of ^{238}U and ^{232}Th by ICP-MS are listed in Table 3. As expected, no events were found in the ROI for 2845 and 352 years of exposure for ^{238}U and ^{232}Th , respectively. For

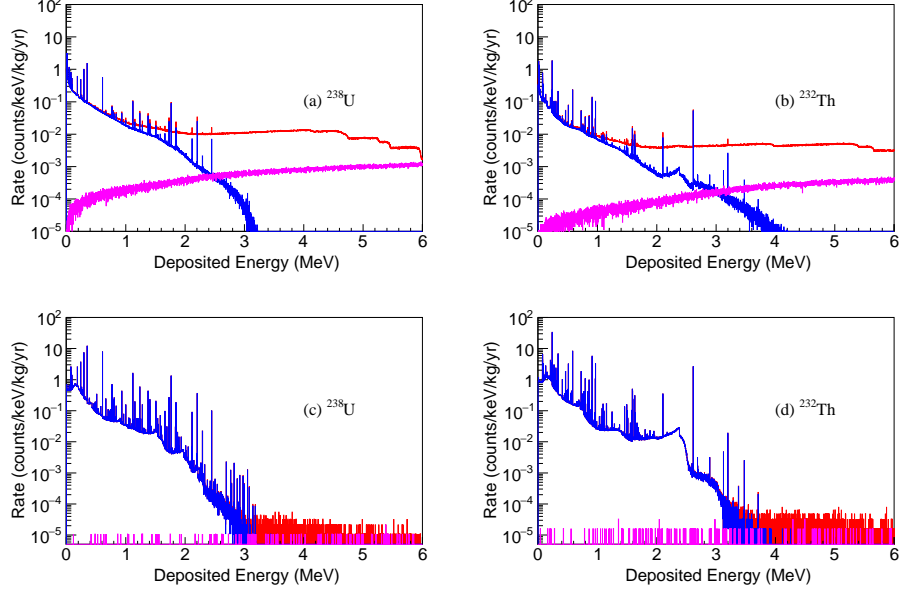


Figure 6: Deposited energy of single hit events from β decay chain (blue) and all decay chains including surface α effect (red) in CMO crystals originated from ^{238}U and ^{232}Th in (a,b) Vikuiti reflector and (c,d) CMO supporting copper frame.

a ^{210}Pb source, 3.3×10^{-7} γ events were expected in the 35 crystals. Considering the ^{210}Pb activity of 59 Bq/kg, 2.6×10^4 γ events were expected a day and the estimated random coincidence rate was 3.4×10^{-6} ckky. The total random coincidence rate of ^{100}Mo $2\nu\beta\beta$ decay for ^{210}Pb , ^{238}U , and ^{232}Th from outer lead shield was 3.6×10^{-6} ckky.

3.3. Backgrounds from rock material surrounding underground laboratory

Similar to the lead shielding box, the random coincidence effect of ^{100}Mo $2\nu\beta\beta$ decay and γ s from the rock were investigated with reported concentrations of ^{238}U and ^{232}Th in rocks at Y2L [23]. The concentration of ^{40}K was 2.44 ppm, calculated with the natural abundance of K in rocks and natural abundance ratio of ^{40}K . As expected, no events were found in the ROI and the estimated

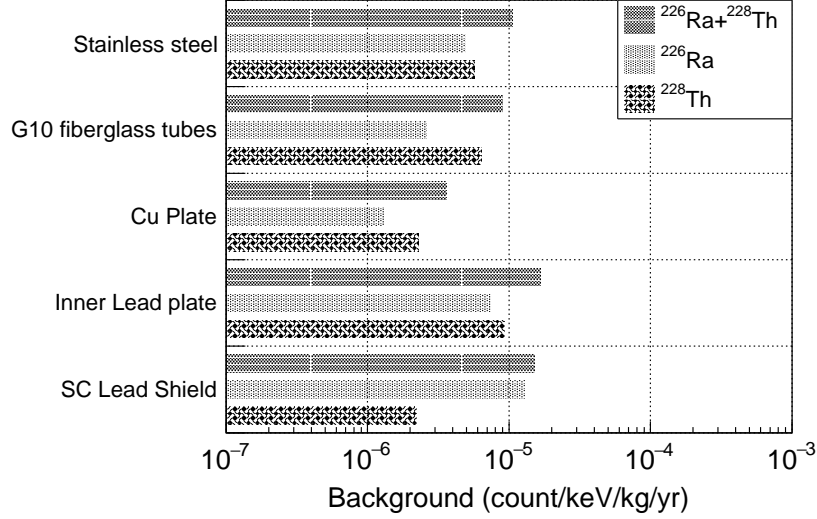


Figure 7: Background β -like event rate of to ^{226}Ra and ^{232}Th in ROI from cryostat and shielding materials.

upper limit (90% C.L.) was 3.3×10^{-7} and 3.7×10^{-7} ckky. The total random coincidence rates of ^{100}Mo $2\nu\beta\beta$ decay with γ -rays from ^{238}U , ^{232}Th , and ^{40}K were

235 9.2×10^{-5} ckky.

3.4. Other backgrounds

- The sandwich panel and cement floor were ones of candidates with relatively high radioactive sources and huge material mass. Concentration of samples of laboratory wall, called sandwich panel, and a cement floor was measured by ICP-MS, listed in Table4. Similar to the effect of rock and the lead shielding box, only γ s make hits on crystals. For instance, for a ^{232}Th source from sandwich panel and cement floor, only $7.4 \times 10^{-7}\%$ events and $9.6 \times 10^{-7}\%$ events appeared, respectively, and no events were in ROI. The estimated random coincidence rate of ^{100}Mo $2\nu\beta\beta$ decays was
- 240
- 245 in the order of 10^{-6} ckky.

Table 4: Concentrations in materials from laboratory environment

	^{238}U	^{232}Th	^{40}K
sandwich panel	1.51 ppm	1.25 ppm	202 ppt
cement floor	2.14 ppm	8.57 ppm	774 ppt

- Other sources of background (cosmogenic ^{88}Y , residual ^{48}Ca in the CMO crystals, and ^{214}Bi in the copper) are not expected to contribute significantly to the background near ^{100}Mo $0\nu\beta\beta$ decay signal region. Nevertheless, they will also be considered in the future.

250 4. Results

The estimated backgrounds of AMoRE-I for possible radioactive sources were summarized in Table 5. The most dominant background source was internal backgrounds in CMO crystals. After applying rejection cuts such as α -tagging method and PSD, β -like event rate from CMO internal background was reduced
255 to $<5.4 \times 10^{-5}$ ckky and $<8.3 \times 10^{-4}$ ckky for ^{238}U and ^{232}Th decay chains, respectively. Vikuiti reflectors and CMO supporting copper frames were the next dominant sources to crystals. After β - α event rejection and ^{208}Tl β rejection methods were applied, the event rate was reduced to $<1.1 \times 10^{-4}$ ckky and $<1.9 \times 10^{-4}$ ckky for ^{238}U and ^{232}Th , respectively, in Vikuiti reflector. The event rate
260 with the rejection method in CMO supporting copper frame was $<2.3 \times 10^{-6}$ ckky and $<2.6 \times 10^{-4}$ ckky, for ^{238}U and ^{232}Th , respectively. In the end, the total expected rate in ROI due to direct background sources were $<1.5 \times 10^{-3}$ ckky.

Estimated random coincidence, listed in Table 6, are random coincidence
265 rate of two ^{100}Mo $2\nu\beta\beta$ decays, as well as that of ^{100}Mo $2\nu\beta\beta$ decays with other radioactive background sources from with possible background sources, including CMO crystals, Vikuiti reflector, CMO supporting copper frames, G10 fiberglass tubes, outer lead shield, rock shell, etc. The most dominant source

Table 5: Summary of α and β -decay-induced (β -like) backgrounds in major components estimated with measurements and simulation. 99.9999% alpha rejection and 90% β - α rejection are assumed.

Background sources	Isotopes	Simulated Time [Years]	Backgrounds in ROI [$\times 10^{-3}$ cnt/keV/kg/yr]			
			α events	β/γ events	β - α pileup	events with cuts
Internal CMO	^{210}Pb	44	17	-	-	-
	^{238}U	34	4.5	-	-	-
	^{226}Ra	520	0.81	0.036	0.19	0.054
	^{232}Th	700	<0.55	<31	<0.15	<0.83
	^{235}U	68	5.5	-	-	-
Vikuiti reflector	^{238}U	2.3×10^4	11	<0.041	<0.66	<0.11
	^{232}Th	4.7×10^4	4.3	<0.17	<0.18	<0.19
CMO supporting copper frame	^{238}U	9.9×10^3	0.013	<0.0022	<0.0013*	<0.0023
	^{232}Th	5.7×10^3	0.020	<0.26	<0.0008	<0.26
SC lead shield	^{238}U	2.6×10^4	-	<0.013		<0.013
	^{232}Th	8.4×10^4	-	<0.0022		<0.0022
Inner lead shield	^{238}U	1.5×10^3	-	<0.0074*		<0.0074
	^{232}Th	1.2×10^3	-	<0.0092*		<0.0092
Cu plate under lead	^{238}U	8.7×10^3	-	<0.0013*		<0.0013
	^{232}Th	2.5×10^4	-	<0.0023		<0.0023
G10 fiberglass tubes	^{238}U	2.4×10^4	-	0.0026		0.0026
	^{232}Th	2.5×10^4	-	0.0064		0.0064
Stainless steel	^{238}U	5.3×10^6	-	<0.0049		<0.0049
	^{232}Th	2.6×10^6	-	<0.0057		<0.0057
Total			<44	<32	<1.2	<1.5

* 90% C.L. with zero-entry

for the random coincidence rate was two ^{100}Mo $2\nu\beta\beta$ decays inside the CMO
 270 crystals, 1.2×10^{-4} ckky. The next dominant background source for the random
 coincidence rate with ^{100}Mo $2\nu\beta\beta$ decay was γ from rock shell, due to its huge
 mass. The total estimated random coincidence rate of ^{100}Mo $2\nu\beta\beta$ decay with
 backgrounds was $<2.3 \times 10^{-4}$ ckky.

Table 6: Backgrounds due to random coincidence with ^{100}Mo $2\nu\beta\beta$ decay

Material	Sources	Random coincidence rate [$\times 10^{-3}$ cnt/keV/kg/yr]
Internal CMO	two ^{100}Mo $2\nu\beta\beta$ decays	0.12
	^{210}Pb , ^{226}Ra , ^{232}Th , ^{40}K , ^{235}U	<0.0078
	two radioactive sources	$<2.2 \times 10^{-5}$
Vikuiti reflector	^{238}U , ^{232}Th	$<1.1 \times 10^{-5}$
CMO supporting copper frame	^{238}U , ^{232}Th	$<3.1 \times 10^{-5}$
SC lead shield	^{210}Pb , ^{238}U , ^{232}Th	$<5.8 \times 10^{-4}$
Cu Plate	^{238}U , ^{232}Th	$<5.8 \times 10^{-6}$
Inner lead shield	^{210}Pb , ^{238}U , ^{232}Th	$<5.0 \times 10^{-6}$
G10 fiberglass tubes	^{238}U , ^{232}Th	4.1×10^{-4}
Outer lead shield	^{210}Pb , ^{238}U , ^{232}Th	<0.0036
Cement floor	2.61 MeV γ (^{232}Th)	0.0017
Sandwich panel	2.61 MeV γ (^{232}Th)	0.0016
γ from Rock	1.76 (^{238}U), 2.61 (^{232}Th)	0.092
	1.46 MeV (^{40}K)	
Total		<0.23

5. Discussion

275 The most dominant background source in ROI is β from ^{208}Tl decay in
232Th chain inside CMO crystals. In this estimation, the ^{232}Th activity inside
crystals, $50\text{ }\mu\text{Bq/kg}$, was originated from the upper limit requirement for crystal
growing. In reality, activity of ^{238}U and ^{232}Th inside crystals in each crystal is
different, so measured activity of each crystal will be used for future work.

280 For future experiment after AMoRE-I, reducing the effect of ^{208}Tl decay
inside crystal is the most important. Therefore, purification of CMO power
and its growing process have been studied. In addition, methods for improving
 α -tagging efficiency of rejecting ^{208}Tl have studied using simulation. When the
internal background level is reduced to the order of 10^{-4} ckky, reducing back-
285 ground effect from radioactive sources from Vikuiti reflector and CMO support-
ing copper frames should be considered as well.

6. Conclusion

We simulated possible internal and external background sources in AMoRE-
I experiment configuration and the estimated total background rate in ROI
290 was $<1.5 \times 10^{-3}$ ckky. The estimated background level of AMoRE-I experiment
will achieve the aimed level, 2×10^{-3} ckky. For AMoRE-I, main background
source was β from ^{208}Tl events inside the crystals and materials nearby crystals.
In order to reduce background rate further, R&D for crystal purification and
material selection are in progress.

295 Acknowledgments

This research was funded by the Institute for Basic Science (Korea) under
project code IBS- R016-D1.

References

References

- 300 [1] R. N. Mohapatra, et al., Theory of neutrinos: A White paper,
Rept. Prog. Phys. 70 (2007) 1757–1867. [arXiv:hep-ph/0510213](#),
[doi:10.1088/0034-4885/70/11/R02](#).
- [2] J. Beringer, et al., Review of Particle Physics (RPP), Phys. Rev. D86 (2012)
010001. [doi:10.1103/PhysRevD.86.010001](#).
- 305 [3] C. Giunti, C. W. Kim, Fundamentals of Neutrino Physics and Astrophysics,
Oxford, UK: Univ. Pr. (2007) 710 p, 2007.
- [4] H. Bhang, et al., AMoRE experiment: a search for neutrinoless
double beta decay of Mo-100 isotope with Ca-40 MoO-100(4) cryo-
genic scintillation detector, J. Phys. Conf. Ser. 375 (2012) 042023.
310 [doi:10.1088/1742-6596/375/1/042023](#).
- [5] V. Alenkov, et al., Technical Design Report for the AMoRE $0\nu\beta\beta$ Decay
Search Experiment [arXiv:1512.05957](#).
- [6] D. R. Artusa, et al., Exploring the Neutrinoless Double Beta Decay in the
Inverted Neutrino Hierarchy with Bolometric Detectors, Eur. Phys. J. C74
315 (2014) 3096. [arXiv:1404.4469](#), [doi:10.1140/epjc/s10052-014-3096-8](#).
- [7] J. W. Beeman, et al., A next-generation neutrinoless double
beta decay experiment based on $ZnMoO_4$ scintillating bolome-
ters, Phys. Lett. B710 (2012) 318–323. [arXiv:1112.3672](#),
[doi:10.1016/j.physletb.2012.03.009](#).
- 320 [8] D. M. Chernyak, F. A. Danevich, A. Giuliani, M. Mancuso, C. Nones,
E. Olivieri, M. Tenconi, V. I. Tretyak, Rejection of randomly coinciding
events in $ZnMoO_4$ scintillating bolometers, Eur. Phys. J. C74 (2014) 2913.
[arXiv:1404.1231](#), [doi:10.1140/epjc/s10052-014-2913-4](#).

- [9] H. J. Lee, J. H. So, C. S. Kang, G. B. Kim, S. R. Kim, J. H. Lee, M. K. Lee, W. S. Yoon, Y. H. Kim, Development of a scintillation light detector for a cryogenic rare-event-search experiment, Nucl. Instrum. Meth. A784 (2015) 508–512. doi:10.1016/j.nima.2014.11.050.
- [10] S. Agostinelli, et al., GEANT4: A Simulation toolkit, Nucl. Instrum. Meth. A506 (2003) 250–303. doi:10.1016/S0168-9002(03)01368-8.
- [11] O. A. Ponkratenko, V. I. Tretyak, Yu. G. Zdesenko, The Event generator DECAY4 for simulation of double beta processes and decay of radioactive nuclei, Phys. Atom. Nucl. 63 (2000) 1282–1287, [Yad. Fiz.63,1355(2000)]. arXiv:nucl-ex/0104018, doi:10.1134/1.855784.
- [12] F. Alessandria, et al., Validation of techniques to mitigate copper surface contamination in CUORE, Astropart. Phys. 45 (2013) 13–22. arXiv:1210.1107, doi:10.1016/j.astropartphys.2013.02.005.
- [13] G. B. Kim, et al., A CaMoO₄ Crystal Low Temperature Detector for the AMoRE Neutrinoless Double Beta Decay Search, Adv. High Energy Phys. 2015 (2015) 817530. doi:10.1155/2015/817530.
- [14] G.-B. Kim, A $0\nu\beta\beta$ search using large scintillating crystal with metallic magnetic calorimeter, Ph.D. thesis, Seoul National University (2016).
- [15] F. Alessandria, et al., CUORE crystal validation runs: results on radioactive contamination and extrapolation to CUORE background, Astropart. Phys. 35 (2012) 839–849. arXiv:1108.4757, doi:10.1016/j.astropartphys.2012.02.008.
- [16] in preparation.
- [17] D. M. Chernyak, F. A. Danevich, A. Giuliani, E. Olivieri, M. Tenconi, V. I. Tretyak, Random coincidence of 2ν 2β decay events as a background source in bolometric 0ν 2β decay experiments, Eur. Phys. J. C72 (2012) 1989. arXiv:1301.4248, doi:10.1140/epjc/s10052-012-1989-y.

- [18] P. Belli, et al., New observation of $2\beta 2\nu$ decay of Mo-100 to the $0^+(1)$ level of Ru-100 in the ARMONIA experiment, Nucl. Phys. A846 (2010) 143–156. doi:10.1016/j.nuclphysa.2010.06.010.
- [19] D. Blum, et al., Search for gamma-rays following beta beta decay of Mo-100 to excited states of Ru-100., Phys. Lett. B275 (1992) 506–511. doi:10.1016/0370-2693(92)91624-I.
- [20] in preparation.
- [21] M. Laubenstein, G. Geusser, Cosmogenic radionuclides in metals as indicator for sea level exposure history, Appl. Rad. Isot. 67 (2009) 750. doi:10.1016/j.apradiso.2009.01.029.
- [22] A. R. Smith, D. L. Hurley, Gamma spectrometric analyses of materials, SNO Technical Reports Rad SNO-STR-91-015 (1991).
URL <http://www.sno.phy.queensu.ca/sno/str/index.html>
- [23] M. Lee, et al., Radon Environment in the Korea Invisible Mass Search Experiment and Its Measurement, J. Kor. Phys. Soc. 58 (2011) 713. doi:10.3938/jkps.58.713.